

Synthesis, Characterization, and Crystal Structure of Cobalt(II) and Zinc(II) Complexes with a Bulky Schiff Base Derived from Rimantadine¹

X. D. Jin^{a,*}, G. C. Han^a, H. M. Liang^a, L. Kou^a, J. Tong^a, K. J. Ren^b, and X. B. Zhao^b

^aCollege of Chemistry, Liaoning University, Shenyang, 110036 P.R. China

^bLiaoning Provincial Institute of Safety Science, Shenyang, 110003 P.R. China

*e-mail: jinxudong@lnu.edu.cn

Received October 16, 2015

Abstract—Two novel complexes, $C_{38}H_{48}CoN_2O_2$ (**I**) and $C_{38}H_{48}N_2O_2Zn$ (**II**), were prepared through an analogous procedure with a corresponding metal chloride and a bulky Schiff base ligand (HL) which derived from rimantadine and salicylaldehyde in appropriate solvents, respectively. They were structurally characterized by the means of IR, UV-Vis, elemental analysis, molar conductance, PXRD and single-crystal X-ray diffraction (CIF files nos. 946735 (**I**), 893304 (**II**)). Single-crystal X-ray diffraction analysis reveals that **I** belongs to the triclinic system, $P\bar{1}$ space group; each asymmetric unit consists of one cobalt(II) complex and one lattice ethanol molecule. In each complex molecule, cobalt(II) atom is four-coordinated via two oxygen atoms and two nitrogen atoms from the deprotonated Schiff base ligands, forming an approximate planar geometry. The crystal structure also involves strong O—H \cdots O intermolecular hydrogen bonds between the solvent alcoholic and phenol O atoms of complex molecule. Complex **II** belongs to the monoclinic system, Cc space group. Each asymmetric unit consists of one zinc(II) ion and two deprotonated ligands. Zinc(II) atom lies on a twofold rotation axis and is four-coordinated via two nitrogen atoms and two oxygen atoms from the Schiff base ligands, forming a distorted tetrahedral geometry.

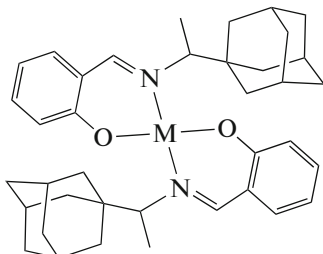
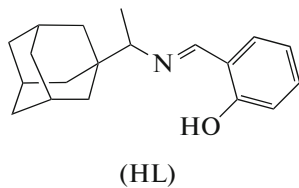
DOI: 10.1134/S1070328416080029

INTRODUCTION

In many countries, amantadine (SymmetrelTM) and rimantadine (FlumadineTM) have been widely used to treat or prevent seasonal influenza as efficacious remedies because they could inhibit the early stages of virus replication by blocking the ion channel, which formed by the M2 protein of influenza A viruses [1–4]. Salicylaldehyde was used to produce effective herbicide, pesticides and fungicide with anti-inflammatory, antibacterial, sterilization and antiviral [5]. Owing to transition metal complexes of Schiff bases play an important role in the field of biochemistry, analysis and antibiosis reagents, they have been widely studied [6, 7]. Zinc and cobalt are vital elements in the organisms and important enzyme active sites, although with lower amounts in most of lives [8–11]. Up to now, a large number of complexes of cobalt(II) and zinc(II) with simple and common ligands, such as water and pyridine have been studied, the trends possessing adamantyl

group of compounds have hardly been investigated. In view of these points above, we designed and managed to synthesize a series of complexes containing both above mentioned metal ions and the ligand derived from rimantadine and salicylaldehyde. As an extension of our previous work on metal complexes with bulky Schiff bases [12, 13], in this paper, two ML_2 coordinated style complexes, which are bis(2-(1-(adamantan-1-yl)-ethylimino-methyl)phenolato- N,O)-cobalt(II) (**I**) and bis(2-(1-(adamantan-1-yl)-ethylimino-methyl)phenolato- N,O)-zinc(II) (**II**) were successfully synthesized from a certain bulky Schiff base ligand—2-(1-(adamantan-1-yl)ethylimino-methyl)phenol (HL) in the presence of NaOH. Their structures were characterized by the means of IR, UV-Vis, elemental analysis, molar conductance, powder X-ray diffraction (PXRD) and single-crystal X-ray diffraction. The antibacterial activities of complexes against two bacteria *Escherichia coli* and *Bacillus subtilis* were simultaneously investigated.

¹ The article is published in the original.



I: M = Co; II: M = Zn

EXPERIMENTAL

Materials and methods. All chemicals and solvents were purchased from Sinopharm Chemical Reagent Co., Ltd., they were analytical grade and used without any further purification. Elemental analysis was carried out on Perkin Elmer Flash EA 1112. Chemical shifts (δ) for ^1H NMR spectra were recorded at 300 MHz on a Varian Mercury-Vx300 spectrometer in CDCl_3 solvent containing TMS as an internal standard. IR spectrum was scanned in the range 4000–400 cm^{-1} with KBr pellets on a Nicolet NEXUS FT-IR 5700 spectrophotometer. UV-Vis spectrum was measured on a Perkin Elmer Lambda 25 spectrophotometer. Melting points were measured on a WRS-1B micro melting point apparatus which were uncorrected. PXRD (RINT 2500, XRD-Rigaku Corporation, Japan) was used to confirm the crystal phase. The molar conductance of the complexes in DMF (1.0×10^{-3} mol L^{-1}) was measured on a DDS-11A conductometer.

Synthesis of HL. A mixture of rimantadine (1.43 g, 8.0 mmol) and salicylaldehyde (0.97 g, 8.0 mmol) in 60 mL anhydrous alcohol was refluxed for 2 h. After reducing the solvent to 20 mL and cooling to room temperature, the precipitated yellow solid was filtered off and dried. The yield of yellow powder was 1.54 g (68%); m.p. 88.0–88.6°C (M.p. 86.0°C [14]). Recrystallization from methanol yielded pure product of HL as yellow needles.

UV-Vis (hexane, $c = 0.67 \times 10^{-4}$ mol/L): $\lambda_{\max} = 255$ (1.156), 314(0.405); $\lambda_{\min} = 277$ (0.113). IR (KBr; ν , cm^{-1}): 3437 w, 2969 w, 2912 s, 2847 m, 1630 s, 1581 w, 1499 w, 1454 w, 1414 w, 1384 w, 1362 w, 1345 w, 1315 w, 1279 w, 1250 w, 1206 w, 1149 w, 1123 w, 1093 w, 1078 w, 1022 w, 974 w, 924 w, 900 w, 867 w, 850 w, 784 w, 768 w, 753 w, 739 w, 644 w, 627 w. ^1H NMR (CDCl_3 ; 300 MHz; δ , ppm): 13.94 (s., 1H, Ar–OH); 8.26 (s., 1H, CH=N); 7.33 (t., $^3J = 7.8$, 1H, Ar–H); 7.25 (d., $^3J = 7.8$, 1H, Ar–H); 6.96 (d., $^3J = 8.4$, 1H, Ar–H); 6.86 (t., $^3J = 7.5$, 1H, Ar–H); 2.84 (q., $^3J = 6.6$, 1H, N–CH); 1.99 (s., 3H, CH, adamantine ring); 1.67 (q., $^3J = 6.6$, 6H, CH_2 , adamantine ring); 1.67 (q., $^3J = 6.6$, 6H, CH_2 , adamantine ring); 1.56 (s., 6H, CH_2 , adamantine ring); 1.18 (d., $^3J = 6.6$, 3H, $\text{CH}_3\text{CH}=\text{N}$).

ring); 1.56 (s., 6H, CH_2 , adamantine ring); 1.18 (d., $^3J = 6.6$, 3H, $\text{CH}_3\text{CH}=\text{N}$).

For $\text{C}_{19}\text{H}_{25}\text{NO}$ ($M = 283.4$)

anal. calcd., %: C, 80.52; H, 8.89; N, 4.94.
Found, %: C, 80.17; H, 8.82; N, 5.21.

Synthesis of complex I. A stirred solution of HL (0.57 g, 2.0 mmol) in 20 mL absolute methanol was mixed with NaOH (0.08 g, 2.0 mmol), refluxed for about 10 minutes. Cobalt(II) chloride hexahydrate (0.24 g, 1.0 mmol) in 20 mL anhydrous methanol was added dropwise to the solution. Then the mixture was refluxed for about 2 h. The powdery precipitates were filtered and dried to afford I as red needles. The yield of I was 0.28 g (45%); m.p. 258.2–259.3°C.

UV-Vis (hexane, $c = 0.25 \times 10^{-4}$ mol/L): $\lambda_{\max} = 248$ (1.272), 311 (0.378), 355 (0.201); $\lambda_{\min} = 283$ (0.272), 353 (0.196). IR (KBr; ν , cm^{-1}): 3438 m, 2905 s, 2846 m, 1600 s, 1532 m, 1451 s, 1323 m, 1189 w, 1142 m, 1082 m, 1027 w, 931 w, 856 w, 749 m, 602 m, 503 m, 456 m.

For $\text{C}_{38}\text{H}_{48}\text{CoN}_2\text{O}_2$ ($M = 623.73$)

anal. calcd., %: C, 73.17; H, 7.76; N, 4.49.
Found, %: C, 73.20; H, 7.73; N, 4.48.

Synthesis of complex II was carried out by following the analogous procedure outlined for I. Cobalt(II) chloride hexahydrate was replaced with zinc(II) chloride (0.14 g, 1.0 mmol), yielding a grey powder. The yield of II was 0.24 g (39%); m.p. 219.7–221.7°C.

UV-Vis (hexane, $c = 0.25 \times 10^{-4}$ mol/L): $\lambda_{\max} = 243$ (1.287), 296 (0.332), 366 (0.296); $\lambda_{\min} = 285$ (0.302), 325 (0.230). IR (KBr; ν , cm^{-1}): 2907 s, 2846 s, 2667 m, 1609 s, 1534 m, 1458 s, 1329 m, 1253 w, 1189 m, 1142 m, 1083 m, 1036 m, 932 m, 857 w, 800 w, 749 m, 642 w, 600 m, 504 m, 454 w. ^1H NMR (CDCl_3 ; 300 MHz; δ , ppm): 8.06 (s., 1H, CH=N); 7.27 (t., $^3J = 8.9$, 1H, Ar–H); 7.10 (d., $^3J = 6.6$, 1H, Ar–H); 6.81 (d., $^3J = 8.7$, 1H Ar–H); 6.59 (t.,

Table 1. Crystallographic data for complexes **I** and **II**

Parameter	I	II
<i>F</i> _w	715.85	630.18
Crystal size, mm	0.40 × 0.30 × 0.20	0.20 × 0.15 × 0.10
Crystal system	Triclinic	Monoclinic
Space group	<i>P</i> 1̄	<i>C</i> c
<i>a</i> , Å	8.9917(5)	12.8752(13)
<i>b</i> , Å	10.5130(7)	22.9116(13)
<i>c</i> , Å	10.7186(5)	12.5412(14)
α, deg	79.486(5)	90
β, deg	78.782(4)	119.602(14)
γ, deg	75.477(5)	90
<i>V</i> , Å ³	952.53(9)	3216.7(5)
<i>Z</i>	1	4
<i>F</i> (000)	385	2070
Index ranges	−10 ≤ <i>h</i> ≤ 10, −12 ≤ <i>k</i> ≤ 9, −12 ≤ <i>l</i> ≤ 12	−15 ≤ <i>h</i> ≤ 9, −26 ≤ <i>k</i> ≤ 27, −11 ≤ <i>l</i> ≤ 14
ρ, g cm ^{−3}	1.248	2.228
μ, mm ^{−1}	0.493	6.158
Reflections collected/unique (<i>R</i> _{int})	5960/3360 (0.0253)	5848/3842 (0.0267)
Data/restraints/parameters	3360/0/224	3842/2/388
GOOF	1.056	0.989
<i>R</i> ₁ /w <i>R</i> ₂ (<i>I</i> > 2σ(<i>I</i>))*	0.0452/0.1153	0.0321/0.0689
<i>R</i> ₁ /w <i>R</i> ₂ (all data)	0.0500/0.1202	0.0384/0.0737
Absolute structure parameter		−0.014(11)

* *R*₁ = Σ||*F*_o|| − |*F*_c||/|*F*_o||; w*R*₂ = [Σ*w*(*F*_o² − *F*_c²)²/Σ*w*(*F*_o²)²]^{1/2}.

³*J* = 7.2, 1H Ar—H); 1.94 (s., 3H, CH, adamantane ring); 1.93 (d., ³*J* = 11.7, 3H, CH₂, adamantane ring); 1.74–1.35 (m., 12H, adamantane ring).

For C₃₈H₄₈N₂O₂Zn (*M* = 630.18)

anal. calcd., %: C, 72.42; H, 7.68; N, 4.45.

Found, %: C, 72.39; H, 7.58; N, 4.43.

X-ray crystallography. The single crystals of two complexes suitable for X-ray analysis were developed from a solution of ethanol-dichloromethane mixture (1 : 1 v/v) by a slow solvent evaporation. The crystallographic data collections for complexes were conducted on a Bruker Smart Apex II CCD with graphite monochromated MoK_α radiation (λ = 0.71073 Å) at 298(2) K for **I** and 293(2) K for **II** using the ω-scan technique. The data were integrated by using the SAINT program, which also corrected the intensities for Lorentz and polarization effect [15]. An empirical absorption correction was applied using the SADABS program [16]. The structure was solved by direct methods using the program SHELXS-97 and all non-

hydrogen atoms were refined anisotropically on *F*² by the full-matrix least-squares technique using the SHELXL-97 crystallographic software package [17]. The hydrogen atoms were generated geometrically. All calculations were performed on a personal computer with the SHELXL-97 crystallographic software package. X-ray structures of two complexes are shown in figure. The details of the crystal parameters, data collection and refinement for **I** and **II** are summarized in Table 1. Selected bond lengths and angles with their estimated standard deviations are given in Table 2.

Supplementary material for structures has been deposited with the Cambridge Crystallographic Data Centre (nos. 946735 (**I**), 893304 (**II**); deposit@ccdc.cam.ac.uk or <http://www.ccdc.cam.ac.uk>).

Antibacterial activity. One Schiff base ligand and its complexes were investigated against a Gram positive and a Gram negative bacterium by inhibition zone method [18]. The compounds were prepared with five concentrations of 1.0 × 10^{−1}, 1.0 × 10^{−2}, 1.0 × 10^{−3}, 1.0 × 10^{−4}, 1.0 × 10^{−5} mol L^{−1} in DMF. The diameters of inhibition zone were measured after 2 days.

Table 2. Selected bond length (Å) and angles (deg) in complexes **I** and **II***

I					
Bond	<i>d</i> , Å	Bond	<i>d</i> , Å	Bond	<i>d</i> , Å
Co—O(1)	1.9072(18)	N(1)—C(7)	1.287(3)	O(1)—C(1)	1.323(3)
Co—N(1)	2.0016(19)	N(1)—C(8)	1.481(3)	O(2)—C(21)	1.386(6)
Angle	ω, deg	Angle	ω, deg	Angle	ω, deg
O(1)CoN(1)	89.45(8)	C(1)O(1)Co(1)	122.33(18)	N(1)CoN(1A)	180.00
O(1)C(1)C(2)	120.0(3)	C(7)N(1)Co(1)	120.41(19)	N(1)C(7)C(6)	126.6(2)
O(1)C(1)C(6)	122.0(3)	C(7)N(1)C(8)	120.0(2)	N(1)C(8)C(9)	113.6(2)
O(2)C(21)C(20)	110.2(5)	C(8)N(1)Co(1)	119.59(16)	N(1)C(8)C(10)	109.7(2)
II					
Bond	<i>d</i> , Å	Bond	<i>d</i> , Å	Bond	<i>d</i> , Å
Zn—O(1)	1.908(2)	Zn—N(1)	2.032(3)	C(1)—O(1)	1.310(4)
Zn—O(2)	1.914(2)	Zn—N(2)	2.040(3)	C(7)—N(1)	1.287(4)
C(8)—N(1)	1.477(5)	C(20)—O(2)	1.306(4)	Angle	ω, deg
O(1)ZnO(2)	117.58(11)	N(1)ZnN(2)	117.77(12)	C(1)O(1)Zn	123.1(2)
O(1)ZnN(1)	96.59(11)	N(1)C(7)C(6)	129.3(4)	C(7)N(1)C(8)	115.7(3)
O(1)ZnN(2)	114.97(12)	N(1)C(8)C(9)	109.2(3)	C(7)N(1)Zn	117.1(3)
O(2)ZnN(1)	116.46(12)	N(1)C(8)C(10)	111.9(3)	C(8)N(1)Zn	127.1(2)
O(2)ZnN(2)	95.06(11)	N(2)C(26)C(25)	129.1(3)	C(20)O(2)Zn	121.1(2)
O(2)C(20)C(21)	120.1(4)	N(2)C(27)C(28)	107.6(3)	C(26)N(2)C(27)	117.1(3)
O(2)C(20)C(25)	123.2(3)	N(2)C(27)C(29)	113.9(3)	C(26)N(2)Zn	116.4(2)
				C(27)N(2)Zn	125.4(2)

RESULTS AND DISCUSSION

The C, H, and N contents both theoretically calculated values and found values are in agreement with the formulae of $C_{38}H_{48}CoN_2O_2$ for **I** and $C_{38}H_{48}N_2O_2Zn$ for **II**. The molar conductance values (Λ_M) are 1.93 and 2.38 S $cm^2 mol^{-1}$ for **I** and **II**, which belong to the complex type of non-electrolytes molecular [19].

In IR spectrum of **I**, the absorption peak at $3438 cm^{-1}$ is attributed to H—O vibration of lattice ethanol. The strongest absorptions at $1630 cm^{-1}$ for ligand and 1600 — $1609 cm^{-1}$ for complexes are the characteristics of the C=N. The absorption bands at $1189 cm^{-1}$ for **I**, $1252 cm^{-1}$ for **II** are the attributions of C—O stretching vibration of phenolic hydroxyls. The absorption peak at $456 cm^{-1}$ for **I** is attributed to Co—O vibration and the absorption peak at $453 cm^{-1}$ for **II** can be identified as Zn—O, indicating that oxygen atoms of the Schiff bases are coordinated to metal ions.

The UV-Vis data reveal that two complexes exhibited similar pattern in the ultraviolet spectra bands but significant changes in visible spectra regions com-

pared to the ligand. Bands at 255 nm for HL, 248 nm for **I** and 243 nm for **II** are attributed to π — π^* transitions of the benzene ring. Bands at 314 nm for HL is attributed to n — π^* transitions of the p — π conjugation. Bands at 311 nm for **I** is assigned to charge transfer transitions from the ligands to Co(II) (n — π^* transition) of N → Co and O → Co. Bands at 296 nm for **II** is assigned to charge transfer transitions from the ligands to Zn(II) (n — π^* transition) of N → Zn and O → Zn. Broad peaks at 355 nm for **I** could be caused by $d \rightarrow d^*$ transition of Co^{2+} and 366 nm for **II** could be caused by $d \rightarrow d^*$ transition of Zn^{2+} , which can not be found in the ligand.

1H NMR data for complex **II** in $CDCl_3$ are shown in Table 3, in which all data for HL are also provided for comparison. The date for complex **I** can not be supplied due to the paramagnetism of cobalt(II). A singlet peak in chemical shift of 13.94 for ligand could be assigned to the phenolic hydroxyl protons. Because of intramolecular hydrogen bond formation of $—CH=N\cdots HO—$, it was observed in low field. While in **II**, the phenolic hydroxyl proton of the ligand is deprotoned as **II** is formed, resulting that neither the single peak of phenolic hydroxyl proton nor specific

Table 3. ^1H NMR data for ligand and complex **II***

Compound	Ar—OH	CH=N	Ar—H	N—CH	Adamantane ring	CH ₃ CH—N
HL	13.94 (s., 1H)	8.26 (s., 1H)	7.33 (t., $^3J = 7.8$, 1H); 7.25 (d., $^3J = 7.8$, 1H); 6.96 (d., $^3J = 8.4$, 1H); 6.86 (t., $^3J = 7.5$, 1H)	2.84 (q., $^3J = 6.6$, 1H)	1.99 (s., 3H, CH); 1.67 (q., $^3J = 6.6$, 6H, CH ₂); 1.56 (s., 6H, CH ₂)	1.18 (d., $^3J = 6.6$, 3H)
II		8.06 (s., 1H)	7.27 (t., $^3J = 8.9$, 1H); 7.10 (d., $^3J = 6.6$, 1H); 6.81 (d., $^3J = 8.7$, 1H); 6.59 (t., $^3J = 7.2$, 1H)		1.94 (s., 3H, CH); 1.74–1.35 (m., 12H)	

* δ in ppm, J in Hz.

intramolecular hydrogen bond signal recognizable. A number of peaks in chemical shift of 7.27–6.59 ppm for **II** could be assigned to Ar—H while these could be observed at 6.86–7.33 ppm for the ligand. The peaks in the range of 1.99–1.56 and 1.94–1.35 ppm for the ligand and **II** are assigned to the —CH and —CH₂ groups from adamantyl. The singlet at 8.06 ppm assigning to —CH=N proton could be recognizable at 8.26 ppm for ligand. The presence of doublet peaks at 1.18 and 1.03 ppm could be assigned to the methoxyl protons.

The crystallographic analysis of **I** reveals that the unit cell contains one complex and two solvent molecules (Fig. 1a). In complex molecule, cobalt(II) atom is four-coordinated via two oxygen atoms and two nitrogen from the deprotonated Schiff base ligands, forming a perfectly plane geometry with the angles of O(1)CoN(1) 89.45(8) $^\circ$. One of the phenyl ring and the symmetry one ($-1 - x, 1 - y, 1 - z$) have a centroid to centroid distance of 4.687 \AA with an interlunar distances of 3.221(1) \AA which means that there is no π — π interaction but maybe an edge to edge interaction. The cobalt being on an inversion center, there is no other

possibility than a *trans* coordination. Owing to the adamantane, the compound is chiral but there is an inversion center on the cobalt(II) atom so it is the *meso* compound containing the two enantiomers *SRSRSSS/RSRSRRR*. Because of the existing of ethanol in the crystal, the structure also involves strong O—H \cdots O intermolecular hydrogen bonds between the alcoholic and phenol O atoms (O \cdots O 2.795(4), H \cdots O 1.99 \AA , angle O—H \cdots O is 168 $^\circ$. In complex **II**, the zinc(II) atom is four-coordinated via two nitrogen atoms and two oxygen atoms from two deprotonated Schiff base ligands, forming a distorted tetrahedral geometry with the smallest angle of O(2)ZnN(2) 95.06(11) $^\circ$ and the biggest angle of N(1)ZnN(2) 117.77(12) $^\circ$. The two phenyl rings are in the intersecting planes with a dihedral angle of 89.39 $^\circ$. The shortest distance between two adamantane carbons from two ligands is 7.669 \AA for C(19)—C(29), indicating a *cis*-coordination of two ligands to zinc(II) atom (Fig. 1b). Complex **II** is found neither intermolecular hydrogen bonding nor π — π interactions existences in stacking. The complex molecules are regularly arranged by weak

Table 4. Inhibitory of compounds against bacteria growth (inhibition zone*/mm)

Bacteria concentration, mol L ⁻¹	<i>Escherichia coli</i>					<i>Bacillus subtilis</i>				
	1.0 \times 10 ⁻¹	1.0 \times 10 ⁻²	1.0 \times 10 ⁻³	1.0 \times 10 ⁻⁴	1.0 \times 10 ⁻⁵	1.0 \times 10 ⁻¹	1.0 \times 10 ⁻²	1.0 \times 10 ⁻³	1.0 \times 10 ⁻⁴	1.0 \times 10 ⁻⁵
HL	9.0	7.0	6.0	6.0	6.0	7.0	7.0	6.0	6.0	6.0
I	10.0	9.0	7.0	6.0	6.0	12.0	8.0	7.0	6.0	6.0
II	10.0	8.0	7.0	6.0	6.0	12.0	11.0	8.0	7.0	7.0

* Filter paper diameter being 6.0 mm.

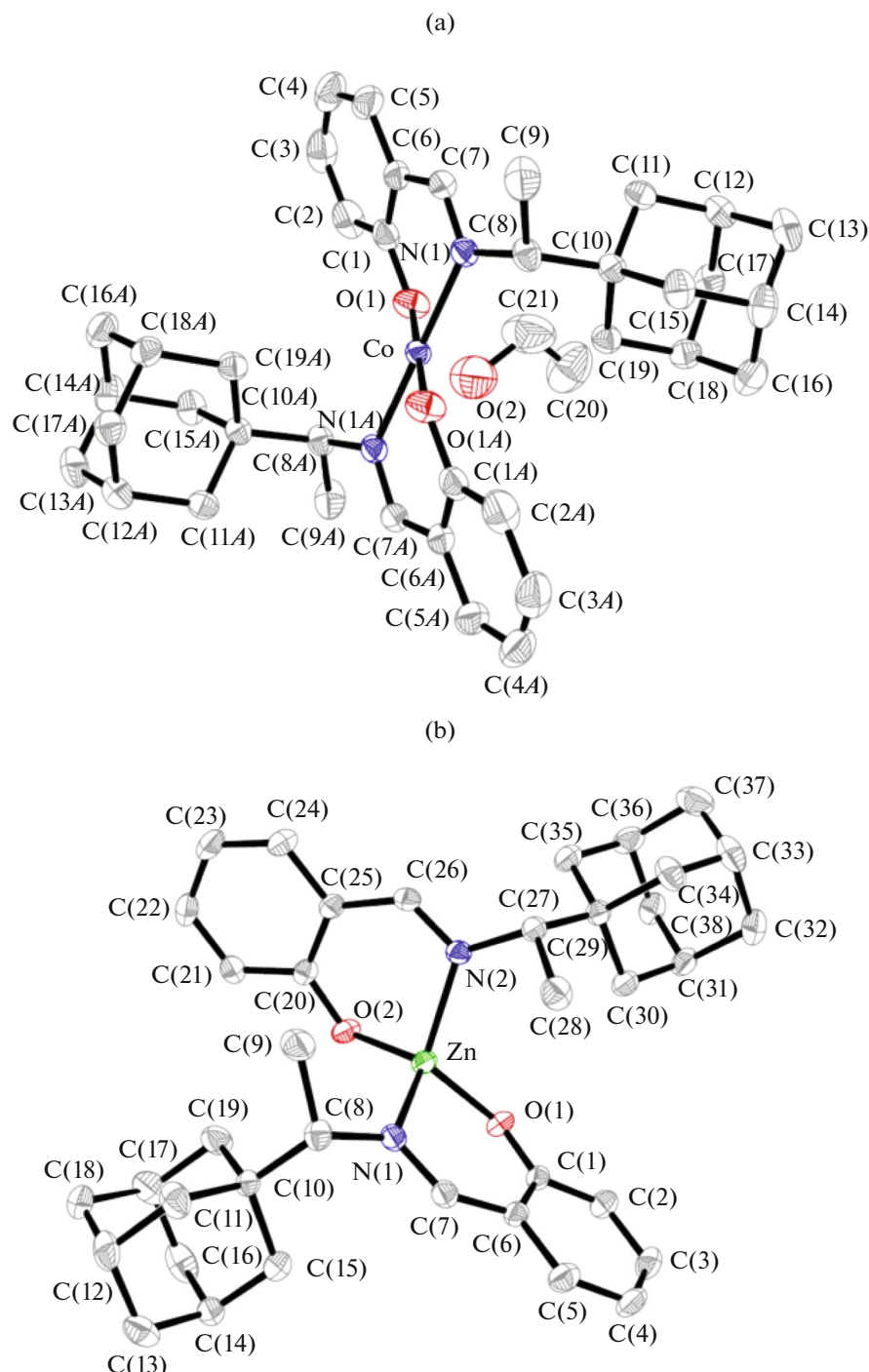


Fig. 1. Diagram of **I** with ethanol (a) and **II** (b), showing 30% thermal ellipsoid. Hydrogen atoms are omitted for clarity. Symmetry operation to display the indexed atoms for **I**: (A) $-x, -y + 1, -z + 1$.

van der Waals forces to construct a net structure containing adamantine cages.

The crystalline structure of **I** and **II** was confirmed by PXRD analysis. The positions of all diffraction peaks in the practical were in good agreement with the peaks in the theoretical. The results indicate that the

products consist of pure phases of **I** and **II** and there are no impurity reflection peaks.

Generally, inhibitory activity of the metal complexes was higher than that of the ligand against both *Escherichia coli* and *Bacillus subtilis*, and antibacterial ability of complexes was in a concentration-dependent

(Table 4). It is worthwhile to note that both the complexes showed the maximum antibacterial effect against *Escherichia coli* and *Bacillus subtilis* in concentrated solution of 1.0×10^{-1} mol L⁻¹, respectively. In contrast with *Escherichia coli*, the complexes demonstrated better antibacterial activity under same testing conditions against *Bacillus subtilis*, and the ligand was not found to have obvious antibacterial activity against *Bacillus subtilis* at above mentioned concentrations.

ACKNOWLEDGMENTS

This work was financially supported by Foundation of Liaoning Provincial Department of Education Innovation Team Projects (LT2015012), the Cause of Public Welfare Scientific Research Fund (2015005008), Shenyang Science and Technology Plan Project (F13-289-1-00).

REFERENCES

1. Pielak, R.M. and Chou, J.J., *Protein Cell*, 2010, vol. 1, no. 3, p. 246.
2. Pielak, R.M., Oxenoid, K., and Chou, J.J., *Structure*, 2011, vol. 19, no. 11, p. 1655.
3. Hayden, F.G., Minocha, A., Spyker, D.A., and Hoffman, H.E., *Antimicrob. Agents Chemother.*, 1985, vol. 28, no. 2, p. 216.
4. Schroeder, C., Möncke-Buchner, H.E., and Lin, T., *Eur. Biophys. J.*, 2005, vol. 34, no. 1, p. 52.
5. Hodnett, E.M. and Dunn, W.J., *J. Med. Chem.*, 1970, vol. 13, no. 4, p. 768.
6. Priya, N.P., Arunachalam, S., Manimaran, A., et al., *Spectrochim. Acta, Part A*, 2009, vol. 72, no. 3, p. 670.
7. Hankare, P.P., Gavali, L.V., Bhuse, V.M., et al., *Indian J. Chem., Sect. A: Inorg., Bio-Inorg., Phys., Theor. Anal. Chem.*, 2004, vol. 43, no. 12, p. 2578.
8. Naumann, C.F., Prijs, B., and Sigel, H., *Eur. J. Biochem.*, 1974, vol. 41, no. 2, p. 209.
9. Burley, S.K., David, P.R., Sweet, R.M., et al., *J. Mol. Biol.*, 1992, vol. 224, no. 1, p. 113.
10. Katakura, R. and Koide, Y., *Chem. Lett.*, 2005, vol. 34, no. 10, p. 1448.
11. Naumann, C.F., Prijs, B., and Sigel, H., *Eur. J. Biochem.*, 1974, vol. 41, no. 2, p. 209.
12. Jin, X.D., Xu, C., Yin, X.Y., et al., *Russ. J. Coord. Chem.*, 2014, vol. 40, no. 6, p. 371.
13. Yang, Q., Xu, C., Han, G.C., et al., *Russ. J. Coord. Chem.*, 2014, vol. 40, no. 9, p. 634.
14. Zhao, G.L., Feng, Y.L., and Liu, X.H., *Wuji Huaxue Xuebao*, 2005, vol. 21, no. 4, p. 598.
15. SAINT, Version 6.02a, Madison: Bruker AXS Inc., 2002.
16. Sheldrick, G.M., SADABS, *Program for Bruker Area Detector Absorption Correction*, Göttingen: Univ. of Göttingen, 1997.
17. Sheldrick, G.M., SHELXS-97, *Program for the Refinement of Crystal Structures*, Göttingen: Univ. of Göttingen, 1997.
18. Bauer, A.W., Kirby, W.M.M., Sherris, J.C., and Turck, M., *Am. J. Clin. Pathol.*, 1966, vol. 45, no. 4, p. 493.
19. Geary, W.J., *Coord. Chem. Rev.*, 1971, vol. 7, no. 1, p. 81.